JURNAL INFOTEL
Informatics - Telecommunication - Electronics
Website Jurnal : http://ejournal.st3telkom.ac.id/index.php/infotel
ISSN : 2085-3688; e-ISSN : 2460-0997

Telemetering of Rainfall Measurement Results Using 433 MHz Wireless Transmission

Hudiono[1]*, Mochammad Taufik[2], Ridho Hendra Yoga Perdana[3], Amalia Eka Rakhmania[4]

[1,2,3,4]State Polytechnic of Malang, Indonesia
[1,2,3,4]Sukarno Hatta Street, No. 9, Malang, East Java, 65141, Indonesia
*Corresponding email: hudiono@polinema.ac.id

Received 17 January 2021, Revised 22 June 2021, Accepted 18 August 2021

Abstract — The line of sight (LOS) microwave communication system, especially those operating at frequencies above 10 GHz, is very susceptible to rain attenuation, particularly in tropical countries like Indonesia. Therefore, it is essential to calculate rain attenuation estimation values as a basis for designing a line of sight microwave communication system to get regular communication. In this study, a telemetering system prototype is proposed to measure rainfall intensity value using the LoRa F8L10D 433 MHz wireless transceiver. Rain gauge is simulated at a distance of 100 meters. The LoRa transceiver range test results can reach up to 200 meters using a small loop antenna and a default transmit power of 17 dBm with a spreading factor of 9. The rain gauge module is calibrated by testing the right and left flip volume balance, with the resolution obtained at 0.03. The telemetering output of the rainfall is displayed in graphical form in real-time, and the measurement results can also be saved in the form of a text data table as a data logger that can be downloaded at any time. The data is used for practical needs in telecommunications engineering laboratories to analyze and calculate rain attenuation values in microwave communication systems.

Keywords – rainfall intensity, rain gauge, line of sight, 433 MHz wireless transceiver.

I. INTRODUCTION

With the increasing need for communication services, the radio spectrum is demanded to have an enormous bandwidth. Thus, the transmission method requires a substantial carrier frequency in the range of more than 10 GHz. Communication systems with very high frequencies are very vulnerable to rain [1]–[3] because it weakens the power received on the receiving side and the communication system's general performance. In addition, raindrops cause scattering and absorption of radio wave energy [4], producing damping called rain attenuation. The amount of rain attenuation depends on the amount of rainfall. The rain attenuation affects the communication system that uses frequencies above 10 GHz [5]–[7]. Rain attenuation can only be determined statistically or in estimated values[8]–[11].

The need for a communication system design, especially for the terrestrial line of sight radio that is reliable and resistant to rain conditions in Indonesia, is essential as Indonesia is a tropical country with very high rainfall; therefore, the damping problems in radio communication links caused by rain are strengthened increasingly. Before the telemetry devices to measure the rainfall from a rain gauge is designed, it is necessary to analyze the characteristics and actual conditions in the field relating to rainfall and the data generated by the rain gauge [12], [13], such as how to collect rainfall data and how to determine the predicted rain attenuation value.

Rainfall is closely related to attenuation as the higher the rainfall will cause higher rain attenuation value[14]; thus, it significantly affects the received power in microwave radio communication systems with a carrier frequency that is above 10 GHz.

In this study, the design and implementation of telemetering devices were carried out due to the direct measurement of rainfall by rain gauge to calculate rain attenuation estimation values in radio communication systems. The measurement results of rainfall were transmitted using a 433 MHz wireless transceiver to the monitoring location to be processed into a graphical display to know in real-time whether the rainfall increases or decreases during the measurement. This device also stored data in the form of a data intensity logger on the hard disk provided to save the results of rainfall measurement whenever the rain occurred.

Several wireless-based transmission technologies have been applied to transmit data from sensor readings located far away in outdoor areas. [15] used the WSN system to monitor the growth of pepper vegetables in a greenhouse. The WSN system presented consists of several sensors distributed around the greenhouse to measure several physical parameters. However, this research is still in concept and has not mentioned the types of wireless technology used. [16] conducted research on hydroponic agriculture using DHT11 sensors, soil moisture sensors, and ultrasonic sensors. This study used sensors to monitor air humidity, temperature, soil humidity, and water in the watering tank. Each data from the sensor is sent to the server via the esp-8266 Wi-Fi module. For a system like this, the location of the sensor must be covered by a Wi-Fi connection. [17] researched security systems and real-time situation monitoring by capturing images using a camera and then transferring these images to the user's mobile device via the GPRS network. However, based on a comparative study of capacity and coverage between LoRa, Sigfox, NB-IoT, and GSM[18], it is revealed that LoRa, Sigfox, and NB-IoT have better performance than GPRS in outdoor conditions.

Research [19] detected and monitored environmental parameters such as temperature and relative humidity in remote areas. This study describes the implementation of a wireless network known as the Low Power Wide Area Network (LPWAN) and explores the performance of LoRa Technology for monitoring system development. Sensor node measurement data is sent to the gateway within 23 km with meager data rates and low power consumption. The proposed system shows that 98% Packet Reception Ratio (PRR) has been successfully received.

Based on previous research, we propose telemetering of rainfall measurement results using LoRa technology type F8L10D with an operating frequency of 433 MHz.

II. RESEARCH METHODS

A rain gauge is a tool used to measure rainfall [20], [21]. The amount of rain that enters a rain gauge is the rainfall representing the area around the measurement. Guidelines issued by WMO (World Meteorological Organization) state that for tropical regions such as Indonesia, a minimum density of 300-1000 km^2 is required for each rainfall station [22]. The rain gauge is a mechanism for recording the amount of rainfall that is automatic. This device records the amount of rainfall at an interval of time and notes the duration of rain. Thus, the amount of rainfall intensity can be determined.

A rain gauge is a device that uses the principle of weighing rainwater in a bucket then channeled with a measuring scale determined based on testing and calibration [23], [24]. The rain gauge has a box that can be made from metal, plastic, and others. When viewed from above, there are filter nets to prevent large-sized objects from entering the bucket. The tipping bucket rain gauge is displayed in Fig. 1.

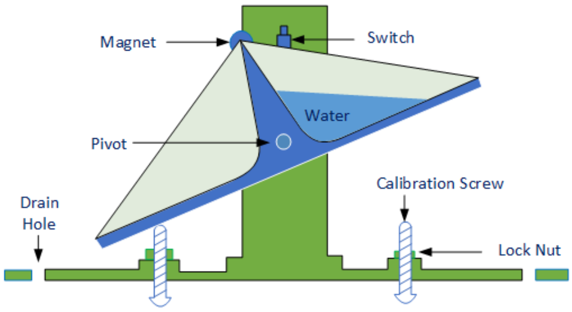

Fig. 1. Tipping bucket rain gauge

In its automatic operation, the rain gauge has mechanically moving components. Raindrops enter through the surface of the measuring funnel, then flow to fill one of the buckets. After every 1.34 mm of raindrops, the bucket will topple, and then the other bucket will be lifted and ready to receive the next 1.34 mm of raindrops. Tipping over the bucket triggers the switch button, and the electronic circuit then records the time in seconds.

A microcontroller does time recording of the tipping bucket. This study used the Arduino Uno microcontroller, an Arduino board that used the ATmega328P microcontroller [25].

Arduino Uno has 14 digital input/output pins (6 pins can be used as PWM output), six analog inputs, a 16 MHz quartz crystal, a USB connection, a voltage source connector, ICSP header, and a reset button. Thus, Arduino Uno contains everything needed to support a microcontroller. The microcontroller works by connecting it to a computer via USB or providing a DC voltage from batteries or an AC to DC adapter. Arduino Uno uses ATmega-16U2, programmed as a USB-to-serial converter for serial communication to a computer via a USB port.

The time data recorded by the microcontroller is based on the RTC (real-time clock) [26], an IC chip functions as a time and data store. There are two types of RTC ICs, namely:

i. DS1307 is a real-time clock (RTC) that uses parallel data lines to store seconds, minutes, hours, dates, months, days of the week, and years up to 2100. It uses 56-byte, batterybacked, RAM nonvolatile (NV) RAM for storage;

ii. DS12C887 uses serial data lines with registers to store data for seconds, minutes, hours, dates, months, and years. This RTC has 128 RAM locations consisting of 15 bytes for time and control data and 113 bytes as available RAM. In addition, DS 12C887 RTC uses multiplexed buses to save pins. Therefore, Intel or Motorola timings can be used to access RTC. The RTC is also equipped with IRQ pins for easy processing.

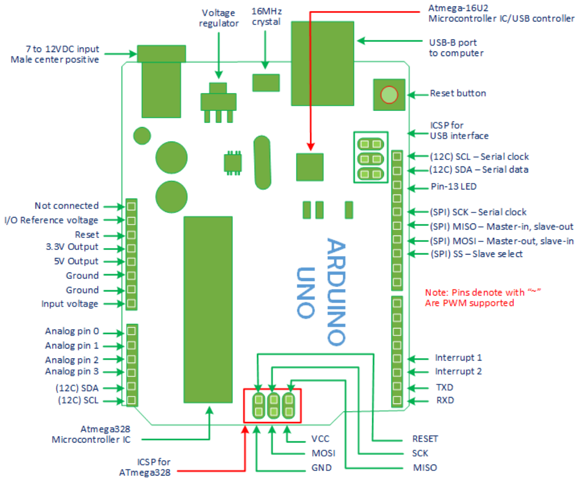

Fig. 2. Output-input pins of Arduino Uno

There are several types of wireless communication; communication networks for short distances that have high data rates (e.g., Wi-Fi), communication systems for short distances and have low data rates (e.g., ZigBee), communications for long distances with low data rates (e.g., LPWAN), and communications for long distances at high data rates (e.g., LTE).

Table 1. The characteristic of existing wireless networks

Wireless System	Long Range, High Data Rate (LTE)	Long Range, Low Data Rate (LPWAN)	Short Range, High Data Rate (WI-FI)	Short Range, Low Data Rate (ZigBee)
Coverage	Large	Large	Small	Small
Range	Long	Long	Short	Short
Latency	Low	High	Low	Low
Power Consumption	Low	Low	High	Low
Operating Cost	Expensive	Cheap	Expensive	Cheap
Topology	Star	Star and Mesh	Star	Point-to-point
Data Rate	High	Low	High	Low

In this study, a LoRa F8L10D type Low Power Wide Area Network (LPWAN) will be used with an operating frequency of 433 MHz, suitable for data telemetering that does not require high speed and low power consumption [27]. Many wireless communication systems with other technologies for telemetering needs, but several challenges are identified as not meeting the application requirements due to several problems such as high cost and high energy, low coverage range [28], and low resistance to interference.

Table 1 shows the comparison between existing wireless networks and LoRa type LPWAN according to [29], [30].

The current requirement for the transceiver can be less than 2uA. Therefore, this transceiver has been widely used for machine-to-machine communication (M2M) such as; transportation supervision, smart grid, industrial equipment automation, telemetry, finance, POS, water supply, environmental protection, post weather, and others.

The wireless transceiver supports Point-to-Point, Point-to-Multipoint, Peer-to-Peer, and Mesh networks, broadcast and target address transfers, wide communication range, and multi I/O channels supply, and it is compatible with analog and digital input.

Fig. 3. Lora 433 MHz wireless transceiver

The study of designing a telemetering system of rainfall measurements by measuring devices using the wireless transceiver 433 MHz was classified into the following stages.

1. Designing and making a rain gauge for direct rainfall measurement, with the generated data to be read by the Arduino microcontroller in the form of sequentially numbered text, the time of each bucket-tipping, and the volume increase of each tipping, which was 1.34 mm.
2. Designing a wireless transceiver for telemetering results of rainfall measurements by the rain gauge.
3. Designing the rainfall telemetering system controls using an Arduino microcontroller.
4. Designing and making software to process rainfall data from the rain gauge into rainfall intensity data R (mm/hour) and displaying it in a real-time rainfall intensity graph, and storing it as a data logger on the provided storage.

The block diagram of the rainfall telemetering device is shown in Fig. 4.

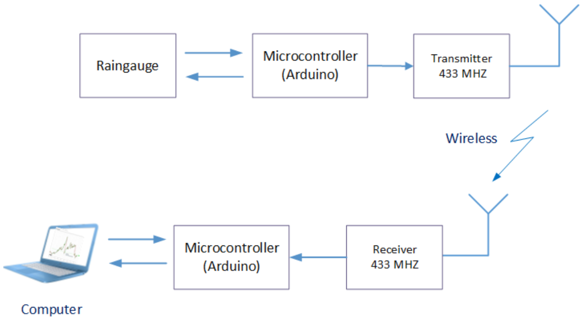

Fig. 4. Block diagram of the rainfall telemetering device

A. *Device Specification*

The rainfall telemetering device consisted of a rain gauge for measuring rainfall, a microcontroller (Arduino), and a wireless 433 MHz transceiver to transmit rainfall measurement results to the monitoring location. Rainfall data received at the monitoring location was processed to obtain the real-time rainfall data.

The specifications of each device are described as follows.

1) *Rain gauge:* This study used a rain gauge with a bucket with a total capacity of 1.34 mm. When the bucket was full, it flipped and caused the magnet to move across the reed switch so that the switch became "short" for a moment. Then, the microcontroller was triggered to record the time of the incident and the volume change of 1.34 mm. The planned output data of the rain gauge was in the form of text, as displayed in Table 2.

Table 2. Rain gauge output data

nth Measurement	Time	Volume
1	14:23:59	1.34
2	14:24:05	2.68
3	14:24:14	4.02
4	14:24:21	5.36
5	14:24:30	6.70
6	14:24:37	8.04
7	14:24:44	9.38
8	14:24:48	10.72
9	14:24:50	12.06
10	14:24:58	13.40

2) *Microcontroller (Arduino Uno)*[25]*:* Arduino Uno was used in the transmitter part (connected directly to the bucket) to control the measurement, process data into data text, and forward it to be transmitted to the monitoring location. Arduino in the receiver also had the same function: control the received data through a 433 MHz receiver to be processed by a computer and displayed in graphical form in real-time and stored as a data logger. The specifications of the Arduino used are described in Table 3.

Table 3. Microcontroller specification

No	Description	Specification
1	Microcontroller	Atmega328P
2	Voltage	7 – 12 V
3	Input	6 – 20 V
4	Digital I/O Pins	14 (6 for PWM)
5	Analog Input Pins	6
6	DC current per I/O	20 mA
7	DC current for 3.3 V Pin	50 mA
8	Flash memory	32 KB with 0.5 KB
9	SRAM	2 KB
10	EEPROM	1 KB
11	Clock	16 MHz

3) *Wireless Transceiver 433MHz*[31]*:* The transceiver used the LoRa module F8L10D type as the primary device to transmit and receive rainfall measurement data by the rain gauge. The specifications of the F8L10D type LoRa transceiver module are shown in Table 4.

Table 4. Specification of lora module f8l10d transceiver

No	Description	Specification
1	Communication Frequency	433 MHz
2	RF LOS range	3500 m
3	Transmit Power	100 mW
4	Digital I/O Pins	14 (6 for PWM)
5	RF Data rate	0.3, 1.2, 2.4, 4.8, 9.6, 19.2 Kbps
6	Receiver Sensitivity	-140 dBm
7	Network Topology	Point to point, point to multipoint
8	Channels	32
9	Antenna Connector	RF, 50 Ohm
10	Power Input	DC 5V/ 1A

4) *User Interface:* The proposed user interface aims to connect the system to users through a web-based application to process rainfall measurement data received at the monitoring location and display the graphical form in real-time. The user interface also stored the data in the form of data loggers.

B. *Data Processing*

Data generated by the rain gauge were texts in the form of flip-times and a volume of 1.34 mm per flip. The data is then converted into the rain rate R (mm/hour) as recommended by ITU. R 838.3 2005 [32]. This process is displayed in Fig. 5.

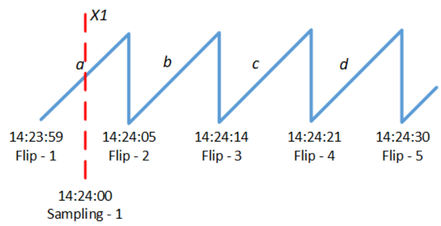

Fig. 5. Calculation of rain rate R (mm/hour)

As shown in Fig. 5, the rain rate of sampling-1 (*X1*) at 14:24:00 was determined using the following equation.

$$X1 = \frac{sampling\ 1 - flip\ 1}{flip\ 2 - flip\ 1}\ x\ 1.34\ \ [mm/min] \quad (1)$$

$$= \frac{14:24:00 - 14:23:59}{14:24:05 - 14:23:59}\ x\ 1.34\ \ [mm/min]$$

$$= \frac{1}{6}\ x\ 1.34\ \ [mm/min]$$

$$= 0.2233\ \ [mm/min]$$

Therefore, the rain rate *R* (mm/hour) of sampling-1 was determined using the following equation.

$$R1 = 0.2233\ x\ 60\ \ [mm/hour] \quad (2)$$
$$= 13.4\ \ [mm/hour]$$

C. System Design

The system design for rainfall telemetering was based on the block diagram in Fig.4. The detailed design of each sub-section is as follows.

1) *Rainfall measurement device:* The rain gauge was controlled by a microcontroller (Arduino Uno) with the design scheme shown in Fig. 6.

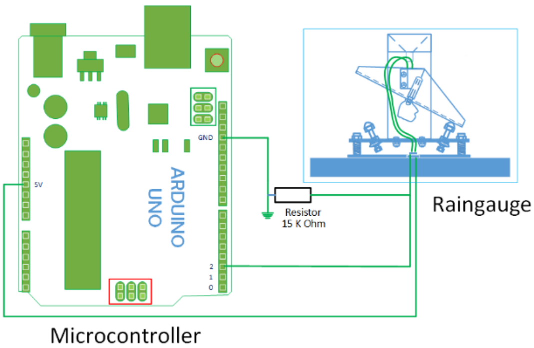

Fig. 6. Rain gauge scheme

2) *Rainfall data transmission:* Rainfall data from the rain gauge were transmitted to the monitoring location using the LoRa Module F8L10D wireless transceiver. The scheme is shown in Fig. 7.

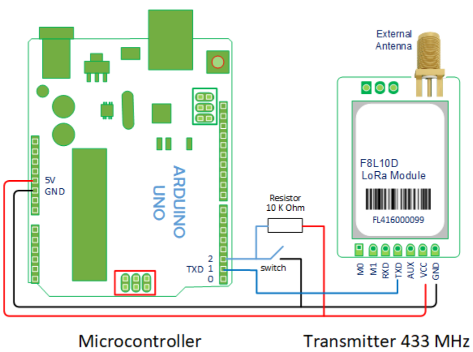

Fig. 7. Scheme of rainfall data transmission circuit

3) *Rainfall Data Receiver System:* At the monitoring location, rainfall data were received using a wireless receiver 433 MHz type LoRa Module F8L10D with the circuit scheme as shown in Fig. 8.

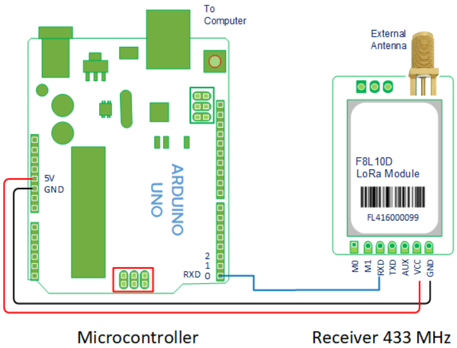

Fig. 8. Rainfall data receiver system

The receiver system was connected to a computer via a USB connector. All rainfall data received then processed by the computer to determine the value of rain rate R (mm/hour) based on Equations (1) and (2) to be displayed in the form of a rain rate table in real-time during the rain. In addition, the data were also displayed in graphical form and stored in the form of rainfall intensity data loggers that can be downloaded at any time.

The rainfall intensity data directly measured by the rain gauge device were processed using a web-based application.

III. RESULTS

The results of this research were the rainfall telemetering device. With this device, rainfall measurement can be done by simply installing the rain gauge in the area where the rainfall is measured. The measurement results can be monitored remotely in real-time or by downloading the data logger of the measurement results.

A. Rain gauge design results

This study used an Arduino-controlled rain gauge that has a bucket with a total capacity of 1.34 mm. The device is shown in Fig. 9.

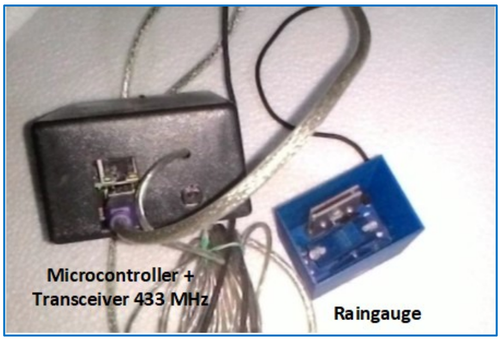

Fig. 9. Controlled rain gauge

The type of rain gauge selected has detailed specifications as follows.

- Type : Tipping bucket
- Output : 0.5 seconds switch closure
- Switch : Sealed reed switch
- Sensitivity : 1 flip per 1.34 mm

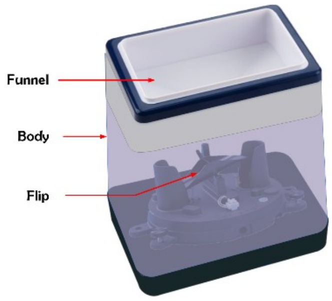

Fig. 10. Raingauge detail specification

- Accuracy : ± 2% up to 2"/hr
- Contact rating : 3 watts, 0.25 amperes, 24 Vdc
- Mounting : 3 feet, ¼" hole bolt diameter

Rain gauge output data is text containing the date, time of measurement, and volume.

B. Rain gauge bucket calibration

The calibration of the rain gauge bucket [33] was done using a measuring cup to measure the volume of water in the bucket. The calibration steps taken were:

a. Prepare 380 ml of water for and pour using a pipette into the tipping bucket for right side flip (right side flip position above)
b. Do ten flips and record the results (10 flips)
c. The remaining water in the tipping bucket is transferred to a measuring cup, and the remaining volume is recorded
d. The same way is done for the tipping bucket with the left side flip (left side flip position on top)
e. Take measurements of each right and left flip five times

Table 5. Results of rain gauge bucket calibration

No	Number of Tipping	Remaining volume with the right flip (ml)	Remaining volume with the left flip (ml)
1	10	1	1.1
2	10	1.3	1.2
3	10	1.2	1.1
4	10	1.3	1.4
5	10	1.3	1.2
Average		$\bar{X} = 1.2$	$\bar{Y} = 1.1$

Based on the tabulated data above, there is a difference in the value of the remaining volume between the left and right flips, which can be solved by adjusting/turning the bolt for balance until the left and right flip bucket volume values are the same.

Then the resolution value of the rain gauge used in this study can be determined as follows:

$$.Resolution = \frac{\bar{X}+\bar{Y}}{2}\ x\ \frac{Tipping\ Amount}{Volume\ of\ water}$$

$$= \frac{1.2+1.1}{2}\ x\ \frac{10}{380}$$

$$= 0.03$$

C. LoRa Transceiver Range Test 433 MHz

The test results are used to benchmark the placement between the rain gauge and the monitoring center. The following are conditions implemented during the test.

a. Tests were carried out in LOS (Line of Sight) conditions
b. Using a measuring tape with an accuracy of 0.5 mm as a distance measuring tool.
c. The RSSI (Receive Signal Strength Indicator) value is measured against the change in the value of the distance between the transmitter and receiver
d. LoRa transmit power is set by default at 17 dBm, with a spreading factor of 9.
e. The position of the transceiver module in the monitoring center is fixed. On the other hand, position in the rain gauge moves away from the receiver per 5-meter scale

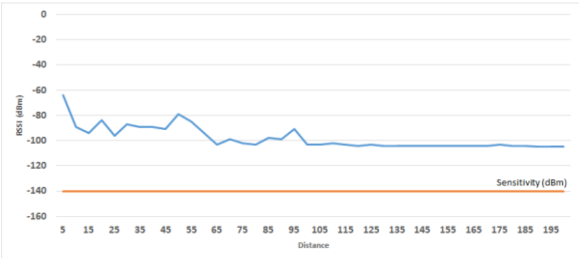

Fig. 11. RSSI value against distance

Tests carried out up to 200 meters, the resulting RSSI value of -105 dBm. Based on the data specification of the LoRa transceiver, it is -140 dBm, so the distance between the rain gauge and the receiver at the monitoring center can reach a distance of up to 200 meters.

In this study, the rain gauge is placed 100 meters from the monitoring center, fixed in position. Monitoring the value of rainfall intensity in real-time is used for practical needs in the Telecommunications Laboratory related to analyzing and determining the value of rain attenuation in the microwave communication system.

IV. DISCUSSION

The rainfall data measured by the rain gauge were transmitted directly through the 433 MHz wireless transceivers to the monitoring location.

The procedure for collecting rainfall data is carried out as follows:

a. Rain gauge, equipped with a control system and 433 MHz wireless transceiver, is placed in an accessible area above the duct, 100 m from the central monitoring room.

b. Rain gauge will record rainfall data based on time and a constant volume increase of 1.34 mm when flipping left, or right occurs
c. A series of time data and volume changes in each flip occurs, directly sent to the server (in the monitoring room)
d. The data received by the server is then processed using special web-based application software to determine the value of the rainfall intensity (rain rate) R based on equations (1) and (2)
e. This rain rate value is then displayed in the form of a graph so that the rain rate data that appears is real-time rainfall intensity data.

Below is a graph of the rainfall intensity values for the three rain measurement conditions, as follows:

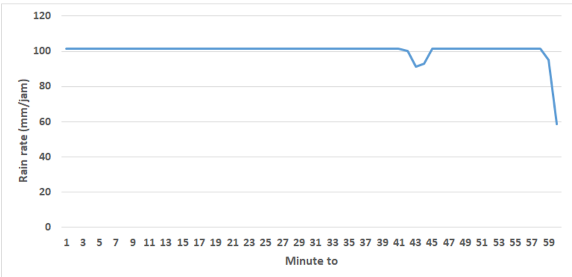

(a) Rain rate for rainfall during the first quarter of the year

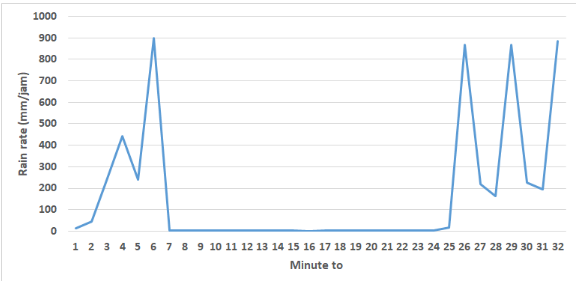

(b) Rain rate for rainfall during the second quarter of the year

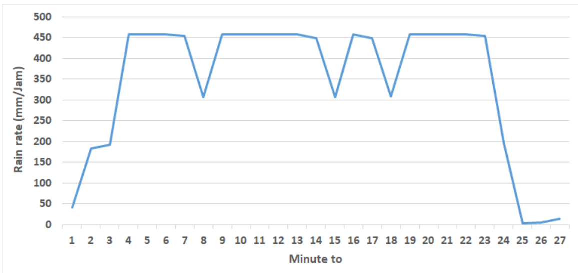

(c) Rain rate for rainfall during the third quarter of the year

Fig. 12. The rain rate value of three rainfall measurement results

V. CONCLUSION

This research proposes a prototype of a rainfall telemetering system simulated at a distance of 100 meters using a LoRa F8L10D 433 MHz wireless transceiver. Based on the test data, this LoRa transceiver range can reach up to 200 meters using a small loop antenna and a default transmit power of 17 dBm with a spreading factor of 9. The comparison device uses a measuring cup with a final resolution is 0.03. The output of rainfall telemetering is displayed in real-time graphical form. In addition, measurement results can be saved automatically in text data tables, which can be downloaded at any time. This data is used for practical needs in the telecommunications engineering laboratory to analyze and calculate the value of rain attenuation in microwave communication systems.

REFERENCES

[1] L. da S. Mello and M. S. Pontes, "Unified method for predicting rain attenuation in satellite and terrestrial links," *J. Microwaves, Optoelectron. Electromagn. Appl.*, vol. 11, no. 1, pp. 01–14, Jun. 2012, doi: 10.1590/S2179-10742012000100001.

[2] A. M. Singh and L. J. Singh, *Development of rain and scintillation models at KU-band in Southeast Asia tropical countries*. 2010.

[3] K. Bhowmick and D. Sarddar, "A New Method of Increasing Received Signal Quality Due to Rain Attenuation in Low Earth Orbit Satellites," *Int. J. Eng. Technol. Res.*, vol. 1, no. 2, pp. 117–122, 2013.

[4] Q. Jing, D. Liu, and J. Tong, "Study on the Scattering Effect of Terahertz Waves in Near-Surface Atmosphere," *IEEE Access*, vol. 6, pp. 49007–49018, 2018, doi: 10.1109/ACCESS.2018.2864102.

[5] I. Shayea, T. Abd. Rahman, M. Hadri Azmi, and A. Arsad, "Rain attenuation of millimetre wave above 10 GHz for terrestrial links in tropical regions," *Trans. Emerg. Telecommun. Technol.*, vol. 29, no. 8, p. e3450, Aug. 2018, doi: 10.1002/ett.3450.

[6] C. Kourogiorgas and A. D. Panagopoulos, "A Rain-Attenuation Stochastic Dynamic Model for LEO Satellite Systems Above 10 GHz," *IEEE Trans. Veh. Technol.*, vol. 64, no. 2, pp. 829–834, Feb. 2015, doi: 10.1109/TVT.2014.2322119.

[7] G. N. Ezeh, N. S. Chukwuneke, N. C. Ogujiofor, and U. H. Diala, "Effects of rain attenuation on satellite communication link," *Adv. Sci. Technol. Res. J.*, vol. Vol. 8, nr, no. 22, pp. 1–11, 2014, doi: 10.12913/22998624.1105138.

[8] U. A. Korai, L. Luini, R. Nebuloni, and I. Glesk, "Statistics of attenuation due to rain affecting hybrid FSO/RF link: Application for 5G networks," *2017 11th Eur. Conf. Antennas Propagation, EUCAP 2017*, no. 1, pp. 1789–1792, 2017, doi: 10.23919/EuCAP.2017.7928821.

[9] D. Nandi and A. Maitra, "Study of rain attenuation effects for 5G Mm-wave cellular communication in tropical location," *IET Microwaves, Antennas Propag.*, vol. 12, no. 9, pp. 1504–1507, Jul. 2018, doi: 10.1049/iet-map.2017.1029.

[10] S. Shrestha and D. Choi, "Rain attenuation over terrestrial microwave links in South Korea," *IET Microwaves, Antennas Propag.*, vol. 11, no. 7, pp. 1031–1039, Jun. 2017, doi: 10.1049/iet-map.2016.0553.

[11] A. M. Al-Samman, M. Mohamed, Y. Ai, M. Cheffena, M. H. Azmi, and T. A. Rahman, "Rain Attenuation

Measurements and Analysis at 73 GHz E-Band Link in Tropical Region," *IEEE Commun. Lett.*, vol. 24, no. 7, pp. 1368–1372, 2020, doi: 10.1109/LCOMM.2020.2983361.

[12] D.-J. Seo and J. P. Breidenbach, "Real-Time Correction of Spatially Nonuniform Bias in Radar Rainfall Data Using Rain Gauge Measurements," *J. Hydrometeorol.*, vol. 3, no. 2, pp. 93–111, Apr. 2002, doi: 10.1175/1525-7541(2002)003<0093:RTCOSN>2.0.CO;2.

[13] I. Paz, I. Tchiguirinskaia, and D. Schertzer, "Rain gauge networks' limitations and the implications to hydrological modelling highlighted with a X-band radar," *J. Hydrol.*, vol. 583, p. 124615, Apr. 2020, doi: 10.1016/j.jhydrol.2020.124615.

[14] Y. Sun, Z. Zhang, and L. Li, "A Satellite Communication Link Rain Attenuation Evaluating Scheme Based on Wide Range of Passive Optical Fiber Rainfall Monitoring System," in *Asia Pacific Optical Sensors Conference*, 2016, p. W4A.63, doi: 10.1364/APOS.2016.W4A.63.

[15] M. Srbinovska, C. Gavrovski, V. Dimcev, A. Krkoleva, and V. Borozan, "Environmental parameters monitoring in precision agriculture using wireless sensor networks," *J. Clean. Prod.*, vol. 88, pp. 297–307, Feb. 2015, doi: 10.1016/j.jclepro.2014.04.036.

[16] J. Pitakphongmetha, N. Boonnam, S. Wongkoon, T. Horanont, D. Somkiadcharoen, and J. Prapakornpilai, "Internet of things for planting in smart farm hydroponics style," in *2016 International Computer Science and Engineering Conference (ICSEC)*, 2016, pp. 1–5, doi: 10.1109/ICSEC.2016.7859872.

[17] J. Surendiran, R. Sridhar, and R. Arya, "GPRS based Monitoring System using Image Sensor," *Int. J. Pure Appl. Math.*, vol. 119, no. 12, pp. 14387–14392, 2018.

[18] M. Lauridsen, H. Nguyen, B. Vejlgaard, I. Z. Kovacs, P. Mogensen, and M. Sorensen, "Coverage Comparison of GPRS, NB-IoT, LoRa, and SigFox in a 7800 km^2 Area," in *2017 IEEE 85th Vehicular Technology Conference (VTC Spring)*, 2017, pp. 1–5, doi: 10.1109/VTCSpring.2017.8108182.

[19] N. A. Azmi Ali and N. A. Abdul Latiff, "Environmental Monitoring System Based on LoRa Technology in Island," in *2019 IEEE International Conference on Signals and Systems (ICSigSys)*, 2019, pp. 160–166, doi: 10.1109/ICSIGSYS.2019.8811066.

[20] A. Gires, I. Tchiguirinskaia, D. Schertzer, S. Lovejoy, and A. Schellart, "Definition and implementation of innovative comparison tools between radar and rain gauge rainfall measurement," *9th Int. Work. Precip. Urban Areas Urban Challenges Rainfall Anal. UrbanRain 2012*, no. December, pp. 38–43, 2017.

[21] E. M. Mangundu, J. N. Mateus, G.-A. L. Zodi, and J. Johson, "A wireless sensor network for rainfall monitoring, using cellular network: A case for Namibia," in *2017 Global Wireless Summit (GWS)*, 2017, pp. 240–244, doi: 10.1109/GWS.2017.8300469.

[22] A. G. Awadallah, "Selecting optimum locations of rainfall stations using kriging and entropy," *Int. J. Civ. Environ. Eng*, vol. 12, no. 1, pp. 36–41, 2012.

[23] K. Ulaganathen and M. S. Assis, "Rain attenuation measurements in Malaysia," in *2015 1st URSI Atlantic Radio Science Conference (URSI AT-RASC)*, 2015, pp. 1–1, doi: 10.1109/URSI-AT-RASC.2015.7303073.

[24] A. A. H. Khan and C. K. Ong, "Design and calibration of tipping bucket system for field runoff and sediment quantification," *J. Soil Water Conserv.*, vol. 52, no. 6, pp. 437–443, 1997.

[25] "Arduino – ArduinoBoardUno (EAGLE files and schematic posted)," 2010. .

[26] W. Gay, "Real-Time Clock (RTC)," in *Beginning STM32*, Berkeley, CA: Apress, 2018, pp. 175–193.

[27] O. Khutsoane, B. Isong, and A. M. Abu-Mahfouz, "IoT devices and applications based on LoRa/LoRaWAN," in *IECON 2017 - 43rd Annual Conference of the IEEE Industrial Electronics Society*, 2017, pp. 6107–6112, doi: 10.1109/IECON.2017.8217061.

[28] M. Rebai, M. Le Berre, F. Hnaien, H. Snoussi, and L. Khoukhi, "A Branch and Bound Algorithm for the Critical Grid Coverage Problem in Wireless Sensor Networks," *Int. J. Distrib. Sens. Networks*, vol. 10, no. 2, p. 769658, Feb. 2014, doi: 10.1155/2014/769658.

[29] M. M. Alsulami and N. Akkari, "The role of 5G wireless networks in the internet-of- things (IoT)," in *2018 1st International Conference on Computer Applications & Information Security (ICCAIS)*, 2018, pp. 1–8, doi: 10.1109/CAIS.2018.8471687.

[30] J. E. Shuda, A. J. Rix, and M. J. Booysen, "Towards Module-Level Performance and Health Monitoring of Solar PV Plants Using LoRa Wireless Sensor Networks," in *2018 IEEE PES/IAS PowerAfrica*, 2018, pp. 172–177, doi: 10.1109/PowerAfrica.2018.8521179.

[31] V. Eremin and A. Borisov, "A research of the propagation of LoRa signals at 433 and 868 MHz in difficult urban conditions," *IOP Conf. Ser. Mater. Sci. Eng.*, vol. 363, p. 012014, May 2018, doi: 10.1088/1757-899X/363/1/012014.

[32] D. Y. Choi, "Rain attenuation prediction model by using the 1-hour rain rate without 1-minute rain rate conversion.," *J. Comput. Sci. Netw. Secur.*, vol. 6, pp. 130–133, 2006.

[33] J. Marsalek, "Calibration of the tipping-bucket raingage," *J. Hydrol.*, vol. 53, no. 3–4, pp. 343–354, Oct. 1981, doi: 10.1016/0022-1694(81)90010-X.